Article

Prediction of gas emission from floor coalbed of steeply inclined and extremely thick coal seams mined using the horizontal sublevel top-coal caving method

Yanwei Hu [a], Gang Wang [a, b, *], Jianqiang Chen [c], Zhiyuan Liu [a], Cheng Fan [a], Qian Cheng [a]

[a] Shandong University of Science and Technology, College of Mining and Safety Engineering, Qingdao 266590, PR China
[b] Shandong University of Science and Technology, Key Laboratory of Ministry of Education for Mine Disaster Prevention and Control, Qingdao 266590, PR China
[c] Shenhua Xinjiang Energy Co., Ltd.
Corresponding author: Gang Wang
Address: Room 108, College of Mining and Safety Engineering, Shandong University of Science and Technology, 579 Qianwangang Rd, Huangdao District, Qingdao 266510, PR China.
Tel: +86-13615327361
E-mail: gang.wang@sdust.edu.cn

Abstract: In the steeply inclined and extremely thick coal seams (SIETCS) mined using the horizontal sublevel top-coal caving (HSTCC) method, the uncertainty of gas emission is a safety threat to the mining operations. In order to reduce the occurrence of accidents, the determination of gas emission is crucial. In this paper, we first proposed a prediction model for workers at the floor coalbed to calculate gas emission on site. We then put forward a finite element numerical simulation for researchers to predict gas emission from the floor coalbed. At last, we measured gas emitted from the floor coalbed of SIETCS in Wudong Coal Mine in a specific mining period and used the data to verify the applicability and accuracy of these two gas-emission prediction methods. The results showed that the gas emission from Wudong Coal Mine was 1.08 m^3/min calculated based on the prediction model and 1.07 m^3/min obtained using the user-defined integration method. Both methods have their own advantages, disadvantages and applicable objects, and are important in predicting gas emission from SIETCS mined using HSTCC method.

Keywords: steeply inclined and extremely thick coal seam; horizontal sublevel top-coal caving; gas prediction; numerical simulation

1. Introduction

Gas emission can cause serious accidents in coal mines and adversely impact the safe production of coal [1-2]. Therefore, the daily monitoring and analyzing the gas emitted from mining face is important for the safe production and management of coal mines [3,4]. Because the fully-mechanized coal mining has high mining intensity, high mining speed and unique mining-induced gas emission and migration, it is important to accurately determine the amount and migration characteristics of emitted gas for improving the safety of coal production. So far, it is widely accepted that gas in the mining face is mainly originated from coal walls, falling coals, goaf and their adjacent coalbeds [5–8].

Statistical data have indicated that steeply inclined and extremely thick coal seams (SIETCS) are mined in more than half of the coal mines in the western provinces of China. The reserve of SIETCS in the Urumqi coalfield located in the southern Junggar Basin, Uygur Autonomous Region of Xinjiang, China, is about 3.6 billion tons, accounting for more than 25% of the total reserve of the same kind of coal in entire China [9]. These SIETCS have very complicated structures and are extremely difficult to mine. At present, SIETCS are commonly mined using the fully mechanized,

 doi:10.20944/preprints201909.0333.v1

horizontal sublevel top-coal caving (HSTCC) method. Wudong Coal Mine, which is considered a representative of this kind of coal mines, along with more than ten others, has been mined by this method. The conventional mining method has many disadvantages such as large mining/caving ratio, great difficulty in roof control, desorption and migration of released gas from the coalbed, more residual coals in the goaf, and use of coal seam as the coalbed of the mining face. All of them together greatly increase the difficulties in preventing and controlling gas emission in the mining face, which frequently result in the occurrence of gas outbursts. However, when the fully mechanized HSTCC method is applied, these disadvantages become more severe.

In recent years, many researches have made great efforts to predict the amount of gas emitted. Permeability of coal seam gas is stress/desorption dependent and may change during the lifetime of the gas reservoir. Salmachi et al. [10,11] studied the permeability change of ultra-deep coal seams in the Cooper Basin by analyzing the transient gas pressure. The pore and fracture structures in the coals are important for gas migration and storage. Wang et al. [12] analyzed pore structure and gas permeability using three-dimensional (3D) reconstruction of CT images. Bi et al. [13] combined the linear and nonlinear fitting algorithms to predict gas emission. Saghafi et al. [14] and Wang et al. [15] proposed that stress, gas pressure and coal properties are the main factors affecting gas emission, based on which, Cheng et al. [16] established a dynamic gas emission prediction model. Yang et al. [4] mapped the time series of gas emission on the polar coordinates and predicted gas concentration in the mining face in an intuitive and concise manner. In addition, other models such as the partial correlation analysis and support vector regression model proposed by Yang [17] and the gray prediction model with fractional order accumulation proposed by Wu et al. [18] also obtained good prediction results. Tutak et al. [19] presented the methodology of using artificial neural networks for predicting methane concentration in one mining area. However, these models are all aimed at coal mines extracted by the conventional mining operations, not suitable for SIETCS. When applying HSTCC method, estimation of gas emission from the lower segments toward the mining face using the above models is difficult and inaccurate. Therefore, new models are needed to predict gas emission from the coalbed of SIETCS mined using HSTCC method.

This paper aimed to develop a prediction model for the amount of gas emitted from the floor coalbed in Wudong SIETCS mined using HSTCC method. Due to the uncertainty of the amount of gas emitted from the floor coalbed, we first proposed a prediction model to calculate gas emission on site and numerically simulated the relationship of gas desorption from the floor coalbed by workers at mining face. We then put forward a finite element numerical simulation for researchers to predict gas emission from the floor coalbed. In order to verify the accuracy of gas concentrations obtained from the two prediction methods, we measured the on-site gas concentrations of both intake and return airways at the initial coal mining stage, determined gas emission from the floor coalbed, and applied the measured data into the two models to verify their accuracy and validity. Overall, the established models can accurately predict gas emission from floor coalbed of SIETCS mined using HSTCC method and has practical significance for the safe mining of SIETCS.

2. Gas emission prediction model and gas migration equation

2.1. Prediction model for gas emission from floor coalbed

SIETCS have complicated stratum structures and are very hard to mine. In Xinjiang, China, this type of coalbed is commonly mined using HSTCC method. Since this mining method utilizes solid coal as its coalbed, the gas emitted from the coalbed is a new source of gas compared with other methods for thin coalbeds.

In fact, gas emission from floor coalbed is due to pressure release during mining, i.e., gas is desorbed from the coal seam and released to the mining face. Therefore, gas emission calculated from the floor coalbed due to gas desorption can be used to predict the gas concentration.

Preprints (www.preprints.org) | NOT PEER-REVIEWED | Posted: 29 September 2019 doi:10.20944/preprints201909.0333.v1

The amount of emitted gas is positively related to the intensity of gas emission, which is expressed by the amount of gas emitted from the coal wall per square meter per unit time. The intensity of emitted gas depends on gas pressure, pore and crack structures, gas adsorption nature, and spatial conditions. Under certain mining conditions, the intensity of gas emitted from coal wall is the function of its exposure time.

According to the theory of gas migration in coal and the actual measurement results, the relationship of the intensity of emitted gas per unit area of the fully mechanized mining face wall to time is as follows:

$$V = V_0 \cdot (1+t)^{-\beta} \tag{1}$$

where V_0 is the initial intensity of gas emission per unit coal wall area, $m^3/(m^2 \cdot min)$; β is the decay coefficient of gas emitted from coal wall, min^{-1}; and t is time, min.

The initial intensity of gas emission, V_0, is shown in the following equation:

$$V_0 = \frac{0.026[0.0004(V_{daf})^2 + 0.16]}{W_0} \tag{2}$$

where V_{daf} is the content of volatile matter in coal, %; and W_0 is the original gas content in the coal seam, m^3/t.

Let *l* be the heading distance per production day, m; and u is the average heading speed of the mining face, m/min. Taking the time of a day as $t=l/u$, min, V is the intensity of gas emission from per unit coal wall area within t, $m^3/(m^2 \cdot min)$, the amount of gas emitted per unit coal wall area accumulated in this time interval is:

$$\mathrm{q} = \int_0^t V dt \tag{3}$$

Joining Eqs. (1) and (2) can find the absolute amount of gas emitted as follows:

$$q = V_0 \left(\frac{(1+\mathrm{t})^{1-\beta}}{1-\beta} - \frac{1}{1-\beta} \right) \tag{4}$$

where q is the accumulated amount of gas emitted from per unit exposed coal body area at the moment t, m^3/m^2.

Hence, the absolute amount of gas emitted from the coalbed can be found as

$$Q = \frac{q \cdot S}{t}. \tag{5}$$

Assuming that the exposure length and the mining face the length in one working day are *l* and *w*, respectively, so the effective exposure area after mining is $S=l*w$ in the time $t=l/u$. Bringing both of them into Eq.(4) can find the following equation:

$$Q = w \cdot u \cdot V_0 \left(\frac{(1+\mathrm{t})^{1-\beta}}{1-\beta} - \frac{1}{1-\beta} \right) \tag{6}$$

Bringing those coalbed's characteristic parameters listed in Table 1 into Eq.(6) may find the predictive amount of gas emitted from the floor coalbed of the mining coalbed to be 1.0802 m^3/min.

2.2. Model development of binary gas transport

2.2.1. Mechanical balance equation

In order to study the effective stress of gas in the coal seam, we first numerically simulated the redistribution of mining-induced stress in the working face according to the actual situation of the Wudong Coal Mine, Xinjiang, China, and then used the boundary coupling method to explore the effective stress distribution in coal. In the simulation, we took the classic in-situ stress model that holds two assumptions, i.e., coal reservoir is a uniform, isotropic, and linear elastic material, and its horizontal strain is constant.

Preprints (www.preprints.org) | NOT PEER-REVIEWED | Posted: 29 September 2019 doi:10.20944/preprints201909.0333.v1

The overlying strata stress can be obtained by the following finite integral:

$$\sigma_v = \int_0^D \rho(D) g dD \tag{7}$$

where σ_v is the overlying stratum stress, Pa, ρ is the density of the overlying stratum, kg/m³, and D is the depth of the object coal seam, m.

Without considering the tectonic stress, the horizontal stress mainly comes from the weight of overlying strata. According to Chen [20], the horizontal stress is described as

$$\sigma_H = \sigma_h = \frac{\mu}{1-\mu}\left(\sigma_v - \alpha P_g\right) \tag{8}$$

where μ is Poisson's ratio, and P_g is the porous pressure, Pa.

The effective stress on the coal seam affects changes in its permeability. The average effective stress (tensile stress is positive) can be calculated from

$$\bar{\sigma} = (\sigma_H + \sigma_h + \sigma_v)/3 + \alpha p_g \tag{9}$$

where α is called the effective stress coefficient or Biot coefficient.

2.2.2. Relationship between porosity and permeability

A relationship between gas content and matrix expansion is assumed to be linear and has been widely used [21-23]. The adsorption-induced volumetric strain can be expressed as follows:

$$\varepsilon_v = \frac{\varepsilon_L P_L p_g}{1 + P_L p_g} \tag{10}$$

where ε_L is Langmuir train coefficient (dimensionless).

The porosity-based Palmer and Mansoori model or P&M model [24,25] is described by:

$$\varphi = \varphi_0 + c_m(p_g - p_{g0}) + (\frac{K}{M} - 1)(\varepsilon_v - \varepsilon_{v0}) \tag{11}$$

where φ is the porosity and its subscript, 0, denotes the reference state; c_m is the compressibility of coal, 1/MPa; K is the bulk modulus, MPa; and M is the constrained axial modulus, MPa.

Using the cubic law of porous media [26, 27] can find the relationship between the permeability and the porosity of coal as follows:

$$k = k_0 \cdot \left[\frac{\varphi_0 + c_m(p_g - p_{g0}) + (\frac{K}{M} - 1)(\varepsilon_v - \varepsilon_{v0})}{\varphi_0} \right]^3 \tag{12}$$

2.2.3. Equation of gas migration in coal body of the coalbed

Gas migration in a coal seam obeys the law of conservation of mass [28,30], that is,

$$\frac{\partial \mathrm{m}}{\partial t} + \nabla\left(\rho_g q_g\right) = 0 \tag{13}$$

where m is the content of gas in the coal, kg/m³; ρ_g is the density of gas, kg/m³; q_g is the velocity of gas seepage flow in the coal, m/s; and t is time variable, s.

Assuming that gas is an ideal gas, its density and pressure meet

$$\rho_g = \beta p_g \tag{14}$$

where β is the compressive coefficient, $\beta = M_g/(RT)$, $kg/m^3 \cdot Pa$.

Coal possesses many pores and cracks, where gas exists at adsorbed and free states. The content of gas in coal seam meets the Langmuir equation and the adsorption and desorption of gas are related to the pressure of gas in the coal seam. Their relationship can be expressed as

$$m=\beta\left(\frac{\phi}{p_{\mathrm{a}}}+\frac{\mathrm{V_L}\rho_s}{\mathrm{P_L}+p_{\mathrm{g}}}\right)p_{\mathrm{g}}^2 \tag{15}$$

where p_a is the atmospheric pressure with value of 1.013×10^5 Pa; ρ_s is the density of the coal seam, kg/m^3; V_L and P_L are two Langmuir constants with units being m^3/kg and MPa, respectively.

Free gas subjected to the pressure gradient performs a linear seepage movement in coal, i.e., obeying the Darcy's law [31]

$$q_g=-\frac{k}{\mu_g}\left(\nabla p_g+\rho_g g\nabla z\right) \tag{16}$$

where μ_g is the dynamic viscosity of gas, Pa·s.

From the above equations, we can obtain the equation of continuity for gas in the adsorption and desorption processes:

$$\beta\left[\frac{\phi}{p_{\mathrm{a}}}+\frac{\mathrm{V_L}\rho_s}{\mathrm{P_L}+p_{\mathrm{g}}}-\frac{\mathrm{V_L}\rho_s}{2(\mathrm{P_L}+p_g)^2}p_g\right]\frac{\partial p_g^2}{\partial t}-\nabla\left(\beta\frac{k_g}{\mu_g}\nabla p_g^2\right)=0 \tag{17}$$

3. Numerical simulation of gas seepage in coal

In order to study the desorption and migration behaviors of gas in the floor coalbed and the mechanism of gas emission from coalbed, we numerically simulated the desorption of gas from the coalbed and gas relief pressure in coalbed using COMSOL Multiphysics, explored pressure relief behaviors, and verified the accuracy of the prediction model.

3.1. Geological settings

We used the coal seam characteristics and model parameters listed in Table 1 to numerically simulate the properties of gas desorption and the absolute amount of gas emitted after coal-seam mining and pressure relief. As shown in Fig. 1, the solid mechanical boundary conditions are the upper load σ_v, and the confining pressures σ_H and σ_h. The bottom of the model is set as roller. Under the mining influence, gas occurrence state of the coalbed changes and its concentration decreases with the interval of extracted sections. The content of gas of the coal seam gradually increases with the burial depth enlarging according to the actual gas content of the Wudong Coal Mine. Therefore, describing the initial gas content of the coalbed at different burial depth in the form of a function should be more suitable for revealing the actual state of gas occurrence. The surface of the coal seam exposed after mining is set under the standard atmospheric pressure. Our calculation scheme is aimed at exploring gas desorption-migration-discharge behaviors at the mining sections of 8 m, 40 m, 80 m and 160 m. The calculation parameters are shown in Table 1.

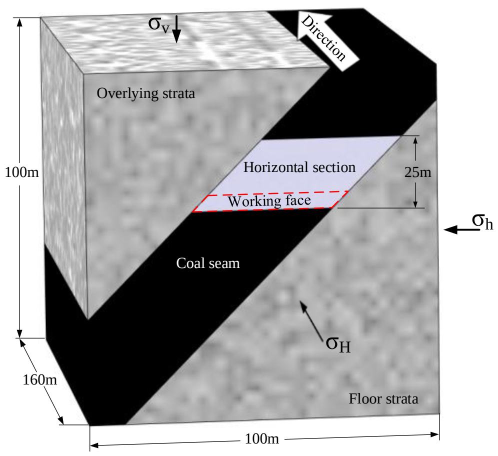

Preprints (www.preprints.org) | NOT PEER-REVIEWED | Posted: 29 September 2019 doi:10.20944/preprints201909.0333.v1

Figure 1. Schematic diagram of geometric model based on Langmuir theory and the geological conditions of Wudong Coal Mine.

Table 1. Coalbed characteristics and model parameters.

Parameter and unit	Value
Coalbed dip, °	45
Face length, m	45
Height of horizontal section, m	25
Decay coefficient, min^{-1}	$3.47e^{-5}$
Content of coal volatile matters, %	29.25
Daily advancing distance, m/d	8
Langmuir volume of methane V_L, m^3/kg	0.025
Langmuir pressure of methane P_L, MPa	1.105
Initial porosity	0.0643
Initial permeability, mD	0.2837
Coal's initial elastic modulus, GPa	3
Strata's initial elastic modulus, GPa	16
Strata's density, kg/m^3	2700
Poisson ratio	0.29
Gas's dynamic viscosity, Pa*s	$1.03e^{-5}$
Standard atmospheric pressure, kPa	101
Molar gas constant, J/(mol*K)	8.314
Standard temperature, K	273.15
Gas density at standard conditions, kg/m^3	0.71068
Molar mass of gas, g/mol	16

3.2. Simulation design

In order to study the amounts of gas emitted from the coalbed of segmentally exploited coalbed and reduce the effects of gas from other sources on the prediction results, we chose the coalbed section adjacent to the ground as our simulation object and ignored gas emission from the roof of the coal seam. Fig.1 shows the geometric model with physical size of 100 m × 100 m × 160 m based on both coal seam gas adsorption-desorption form in the Langmuir theory [31] and the geological conditions of Wudong Coal Mine.

The tetrahedral meshes were selected to enable user-controlled meshing and fluid dynamics was used to calibrate mesh dimensions. There were 318,030 elements in the entire geometry with averaged element quality of 0.6767, as shown in Fig. 2

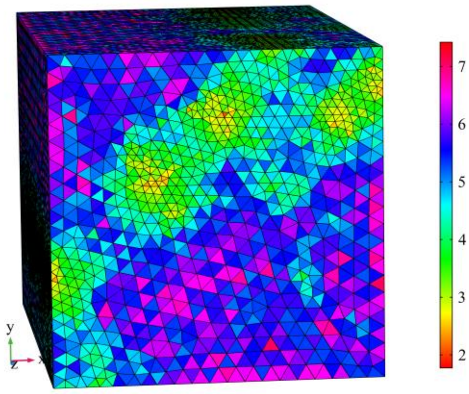

Figure 2. Calculation model and mesh generation.

3.3. Analysis of effects of coal seam's burial depth on its gas occurrence

Because mining the upper section of the coal seam changes permeability of the pressure relief zone, the content of coal seam gas of Wudong Coal Mine increases with the increase of the burial depth. For this reason, we specifically analyzed the occurrence of gas in the No. 45 coal seam of the

 doi:10.20944/preprints201909.0333.v1

Wudong Coal Mine based on geological exploration results and actual underground measurements. Table 2 lists the related gas content data obtained in the No. 45 coal seam

Table 2. Gas content of the 45# coal seam.

Test site and borehole number	Sample burial depth (m)	Gas content (m^3/t)	Notice
+620 Horiz. 45# coal seam. South lane excavation face 1	160	1.98	Underg.test
+620 horiz. 45# coal seam. South lane excavation face 2	173	1.4	Underg.test
+620 horiz. 45# coal seam. South lane excavation face 3	266	3.02	Underg.test
+500 m Horiz. 43#–45# coal seam. Crosscut	280	5.08	Underg.test
+500 m Horiz. 43#–45# coal seam. Crosscut	280	6.43	Underg.test
19-02	499.06	7.02	Geoprospect
19-04	503.02	7.41	Geoprospect
23-01	587.04	9.62	Geoprospect
23-03	589.64	10.16	Geoprospect
27-02	678.8	10.58	Geoprospect
27-04	683.04	10.61	Geoprospect

Fig.3 shows the content of gas in the pressure-relief coalbeds of SIETCS mined using HSTCC method is linearly related to the buried depth. Therefore, initial values were interpolated into the calculation model to describe the occurrence state of gas in the coal seam.

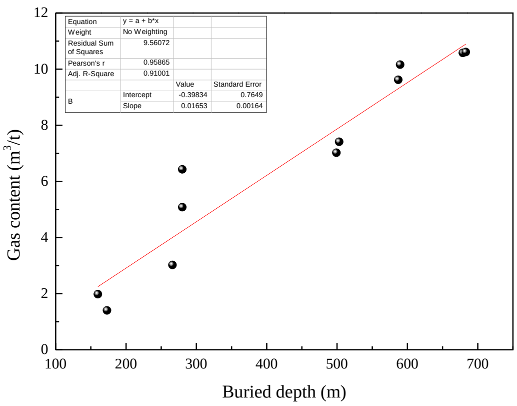

Figure 3. Relationship of gas content to burial depth.

3.4. Simulation results and analysis

The coupling mode between ground stress and coalbed gas can be used to study the mechanisms of how the effective stress affecting coalbed gas adsorption, desorption, compression, and seepage-stress coupling, and further affecting coal seam permeability. In this report, we focus on how the effective stress affecting the permeability of coal seam by taking the mining section from 0 m to 80 m as an example. Fig.4 shows the simulated stress distribution in coal rock strata subject to HSTCC and reflects changes in permeability caused by effective stress. It is clear that due to mining, stress in the coalbed increases and concentrates on the interface between coal seam and surrounding rocks. Fig.5 shows the simulated transfer of effective stress in the coal seam and clearly reflects its magnitude and direction. It can be seen that the distribution of effective stress obviously affects the distribution of coal seam permeability.

Preprints (www.preprints.org) | NOT PEER-REVIEWED | Posted: 29 September 2019 doi:10.20944/preprints201909.0333.v1

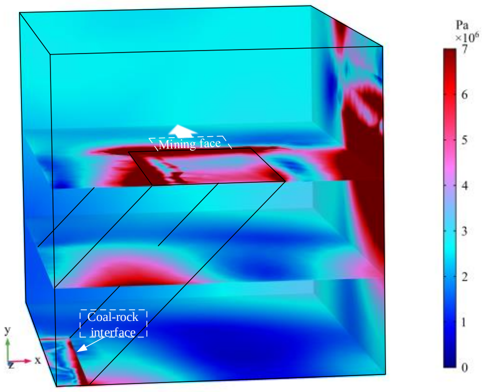

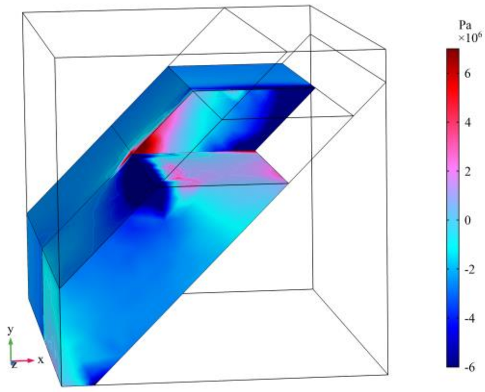

Figure 4. Sectional diagram of stress distribution. **Figure 5.** Distribution of effective stress in coal body.

Fig.6 shows the effect of mining on coal seam permeability. In order to clearly observe the permeability trend in the horizontal direction, four measurement lines are selected in Fig.6(a) to extract the specific permeability along these lines. From the horizontal measurement lines, Line 1, Line 2 and Line 3, as shown in Fig.6(b), permeability has a greater variation in the inclined direction of the coal seam only on the exposed surface of the coal seam. In this figure, when the rock stratum direction adjacent to the upper part of the coal seam is set as the left direction and the rock stratum direction adjacent to the lower part of the coal seam is set as the right direction, it is found that the stress caused by conformation of SIETCS changes coal's permeability, resulting in the increase of permeability of the coalbed from left to right. And the permeability of the upper rock in the left coal seam changes faster.

For the downward measurement line of the horizontal coal seam, it is clear that the permeability along Line 4 in Fig.6 (b) shows a trend of decrease after increase before 20 m and stabilizes at the original level after 20 m. Hence, changes in permeability of coal seams 45 m downward are sufficient to reflect changes in permeability of the coalbed. It is of little significance continually studying change in permeability of deeper coalbeds.

In the downward direction along the coal seam, the permeability increases rapidly in the coalbed 2 m above the exposed surface, affected by the mining of working face, and decreases in the coalbed below 2 m. The influence range to increase permeability is about 20 meters. Therefore, it can be inferred from the coal seam permeability that gas in the range of 20m is rapidly desorbed in the coalbed and rushes to the coal mining face.

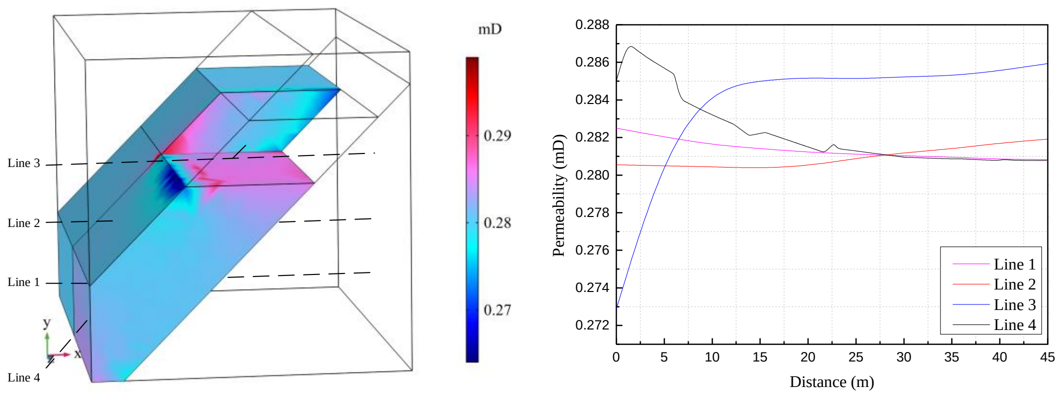

Fig.6 Permeability distribution in coal body at the coalbed. (a) Spatial distribution of permeability of coal seam; (b) Distribution of permeability with the distance at different measurement lines.

 doi:10.20944/preprints201909.0333.v1

Fig.7 shows the gas pressure distribution in coal seams at different mining stages simulated at mining speed of 8 m/d. Clearly, the pressure-relief speed of coalbed along the two sides of the coal bodies in the oblique direction of the coal seam is asymmetric in nature. Near the right side of the coalbed, gas pressure-relief speed is significantly higher than that near the left side close to the top coal stratum. This is consistent with the permeability distribution obtained in previous analyses. With the increase of coal's exposure time, gas desorption speed is faster in the right floor coalbed with higher permeability than in the left coalbed. This fact can be used for selecting the working face intake and return airways during mining of SIETCS using HSTCC method.

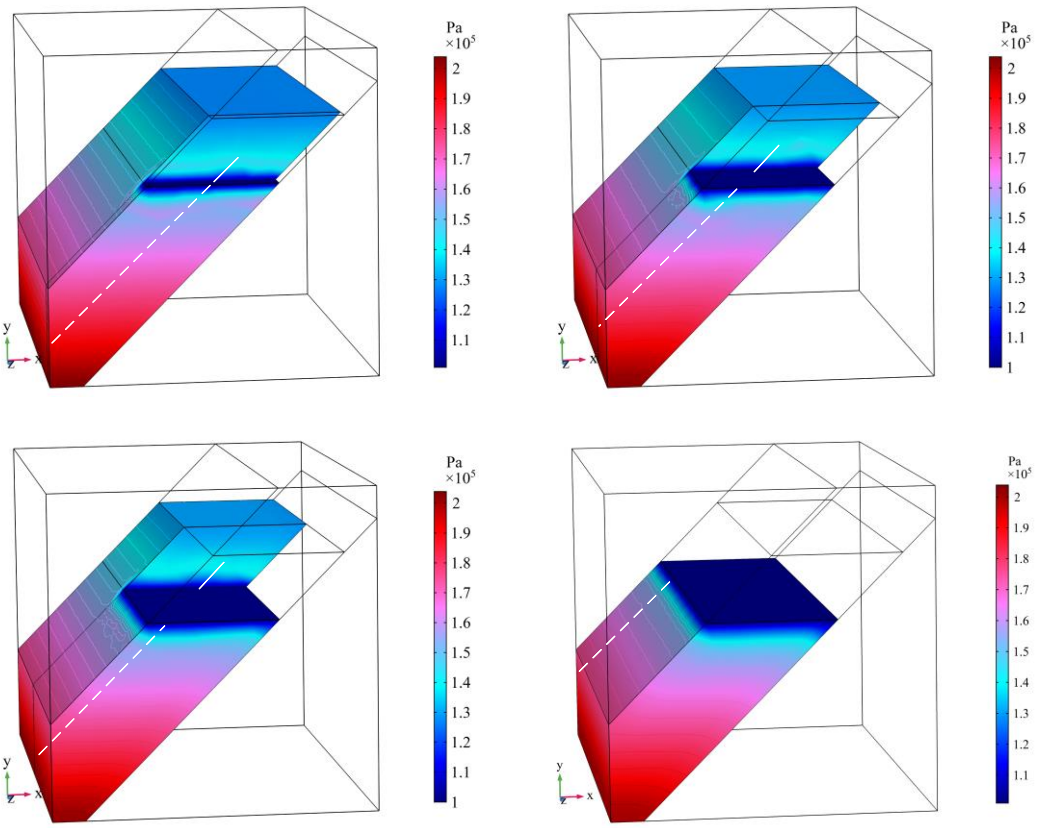

Fig.7 Gas pressure distribution map in coal seam mined to different stages. (a) At day 1 with mining distance of 8 m; (b) At day 5 with mining distance of 40 m; (c) At day 10 with mining distance of 80 m; (d) At day 20 with mining distance of 160 m.

Fig.8 shows the distribution of gas pressure with mining depth at different mining times based on the initial gas pressure data and the measurement lines given in Fig.7. In Fig.6, the coal mining face is located at x=0, and the direction of x-axis is along the coal seam's deepening direction. A total of 5 gas pressure distribution curves are given including the initial gas pressure curve without mining disturbance and 4 gas pressure curves corresponding respectively to the 4 measurement lines at different mining stages given in Fig.7. Through these curves, one can quantitatively study the gas pressure distribution in the coalbed at different mining stages. It is clear from the figure that on the first day of mining, the coalbed rapidly depressurizes within 10 m downward from the horizontal direction of the working surface; On the 5th day, as the face advances to 40 m, the pressure relief range of the coalbed expands to 15 m; On the 10th day, as the face advances to 80 m, the gas pressure relief range increases to 25 m, which coincides with the range at original gas pressure. The gas pressure in the floor coalbed is higher than the initial gas pressure in pressure relief range of 6 m to 18 m on the 1st day, 9 m to 20 m on the 5th day, and 12 m to 22 m on the 10th day. This phenomenon can be explained as that during mining, the gas desorbed from the lower coal body of the coalbed migrates upward. Due to the permeability distribution mentioned above, in about 20 m downward range in the floor coalbed, with the increase of both coal permeability and porosity, the amount of gas accumulated in this segment of coalbed consecutively increases, resulting in a higher gas pressure over the initial gas pressure. On the 20th day of mining, as the face heads to 160 m, the pressure relief range of the coalbed tends to stabilize after 30 m due to mining. With the extension of coal's exposure time, gas desorption rate from coalbed gradually decreases. Thus, the depressurized curve coincides with the original gas pressure curve. At this time, it is not necessary to continually study the pressure relief time, which is consistent with the conclusion obtained from the previous prediction model that the intensity of gas emission from coalbed increases over time while the desorption intensity of coal seam gas reduces.

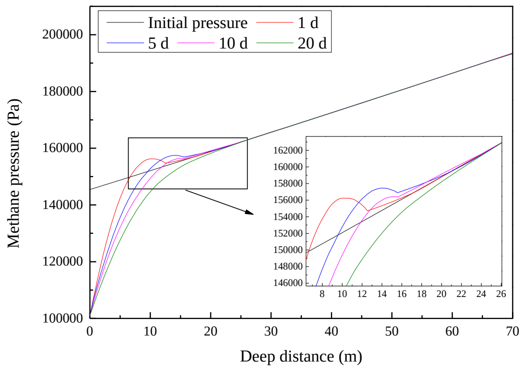

Figure 8. Changes of gas pressure with mining distance over time.

Let the original amount of gas existing in coal seam be m0. From Eq.(15) it is known that the mining-induced gas adsorption amount is m. The finite element numerical simulation shows that all desorbed gas flows to the working face, so the gas emission (m0-m) divided by the gas density in the standard conditions (ρ_a) is the emission volume. Thus, we can find the integral equation used to calculate the absolute gas emission from the 3-dimensional coalbed per unit time as follows:

$$Q=\iiint \frac{m_0\text{-}m}{\rho_a \cdot t}\, dxdydz \tag{18}$$

where Q is the absolute gas emission, m³/min; ρ_a is the density of gas in the standard conditions; and t is the time, min.

From the point view of mining-induced gas desorption from coalbed, we can get the amount of gas emitted from coalbed per unit time. Given that coal mining time is one day, using the user-defined integral Eq.(18) in the calculation model, we first work out the amount of gas emitted from the floor coalbed, then numerically compute the desorption rate of gas within this mining stage, as shown in Fig.9 and Fig.10, and at last find the absolute gas emitted in the mining face within one mining day is 1.07 m³/min.

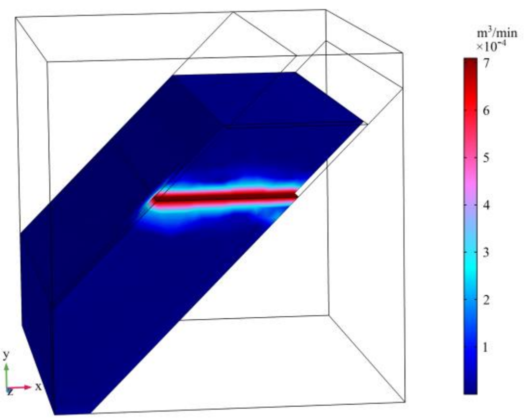

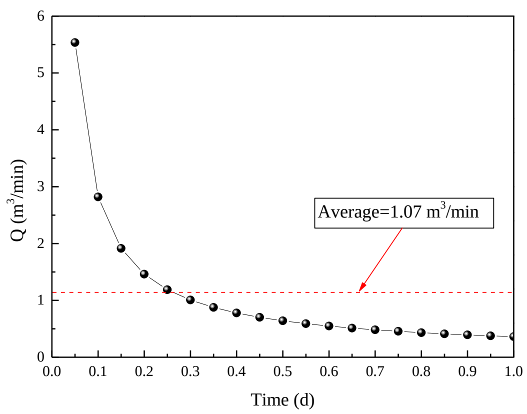

Figure 9. Spatial distribution of gas desorption rate from coalbed at day 1.**Figure 10.** Relationship of gas emission with time.

Preprints (www.preprints.org) | NOT PEER-REVIEWED | Posted: 29 September 2019 doi:10.20944/preprints201909.0333.v1

4. Measured gas emission and error analysis

As described above, we have worked out how to predict the amounts of gas emitted from the face of floor coalbed using our self-built geometrical prediction model and finite element simulation method. In the following sections, we utilize the measured data of Wudong Coal Mine to analyze and discuss the error, accuracy and applicability of these two prediction methods.

4.1. Geological background of Wudong Coal Mine

Wudong Coal Mine is located in Xinjiang, northwest China. Its geographical location is shown in Fig.11. Due to its specific SIETCS, the coal mine adopted the fully-mechanized HSTCC method and complete in-caving method for coal seam roof management. The working face length is 45 m, and the height of the vertically minable section is 22–25 m (with the design mining/caving ratio of 1:7–1:8). The designed mining length is 1124 m. The ground elevation is +739.2–+934.0 m. The mined coal seams mainly include No. 45 and No. 43 coal seams with averaged thickness of 30 m and dip of 45°. The face has simpler geological structure with small folds, fractures and joint development zones, but not large faults and tectonics. The coal seams are fragmentized and prone to cave in. The average coal seam thickness is 30 m and the inclination angle is 45°.

Figure 11. Coal mining and gas measuring methods used at Wudong Coal Mine.

4.2. Gas emission

At the initial excavation period, there is little or no goaf behind the working face. Therefore, during that period, the gas flowing into the face mainly includes those emitted from the front coal wall and the fractures coal seam, as well as those released and desorbed from the coal body in the coalbed. During its overhaul period, the face stops production and no gas was emitted from the fractured coal seam. Therefore, gas in the working face during the overhaul period is only from the front coal wall and the coal body in the coalbed. In order to estimate gas concentration at this period, gas content in the intake and return airways, C_{in} and C_{out}, were measured on site using the differential gas-source-fixing method for a total of 35 days. Statistical analysis showed that the average air volume in the intake and return airways was 858.06 m^3/min and 979.14 m^3/min, respectively. The total gas emission at corresponding period was calculated as the sum of the two, i.e.

$$Q=C_{out}\times V_{out}-C_{in}\times V= 1.5482\ \text{m}^3/\text{min}$$

Fig.12 shows the curves of gas concentration and emission in both the intake and return airways.

Because Wudong Coal Mine adopts HSTCC method, the height of the coal wall exposed in front of the working face is about 4 m and the average length of the exposed coal body at the coalbed is 8 m per day. According to the numerical simulation results in Section 4, it follows that the gas emission from both the exposed front coal wall and the coalbed has similar characteristics. Therefore, the ratio of the two gas sources in the initial mining stage can be determined from the proportion of their exposed areas:

$$Q_{bottom} = \frac{8}{4+8} \cdot Q = 1.032 \text{ m}^3\text{/min}$$

Although this method can be used to accurately estimate gas emission from the coalbed, it is only applicable to a specific mining period. Because of this great limitation, the method can be only used to verify the accuracy of the proposed gas emission prediction model.

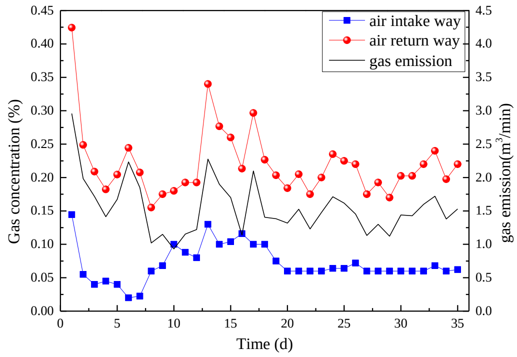

Figure 12. Concentration and amount of gas emission in both intake and return airways.

4.3. Error analysis

Table 3 shows the results of using the measured data to verify both prediction model and simulation method. From the table it is clear that the error of the proposed prediction model is smaller and the predicted value is very close to the actual measurement result. The time-dependent gas emission obtained through the finite-element numerical simulation changes dynamically in a gradually decreasing manner. At ideal conditions, due to the impact of mining on the coal body in the coalbed, the fully desorbed gas from the mining-disturbed coalbed wholly flows into the working face in a working day. Thus, the finite element simulation result is greater than the actual measurement result. Therefore, the gas emitted from floor coalbed predicted using these two prediction methods is slightly greater than that measured in the field and has relatively small errors. In other words, these two methods can be applied to more accurately determine the gas emission from the coalbed of SIETCS mined using HSTCC method and both methods can be used to prevent and control gas disasters.

The above verification shows that the errors between field test results and the prediction model results or the numerical simulation results are within 5%, as shown in Table 3. Therefore, the proposed methods are suitable for calculating gas emission from the coalbed of SIETCS mined using HSTCC method, and have certain scientific significance for studies on the gas emission from coalbed and for gas disaster prevention and control technologies.

Table 3. Comparison and analysis of predicted gas emission.

Prediction method	**Gas emission (m^3/min)**	**Error relative to spot test results (%)**	**Advantage**	**Disadvantages**
Prediction model	1.0802	4.67	Easy use, strong practicality, simple process	Only applicable for predicting gas emission from SIETCS mined using HSTCC method
Numeric simulation	1.07	3.68	Suitable for predicting the amount of gas emission at	Highly depending on the accuracy of the on-site parameters, not

			different times and studies on the law of gas migration in floor coalbed	suitable for miner use.
Spot measurement	1.032	/	Highly accurate	Only effective at specific mining stage, not suitable for general application

5. Conclusions

In order to find the amounts of gas emitted from coalbed of SIETCS during mining using HSTCC method, we constructed a prediction model for gas emission from the coal body in the coalbed. Based on the Langmuir theory, we also set up a 3-dimensional numerical model for gas adsorption-desorption-seepage emission from the coalbed. In addition, we used a self-defined integral method to compute gas emission and verified the rationality and accuracy of the two prediction results through the field measured data. We arrived at the following conclusions.

1) Through analyzing different gas sources in the working face, a method for quantitative prediction of gas emission from coalbed was presented by actually measuring the gas concentrations at the intake and return airways of SIETCS. The measured gas emitted from coal body of the coalbed was 1.032 m^3/min. However, this method has its limitation. It can only be used to verify the accuracy of the prediction models and is not suitable for general applications.

2) A prediction model was proposed to predict gas emission from the coalbed of SIETCS mined using HSTCC method. The emitted gas calculated using the method from the coalbed of SIETCS of Wudong Coal Mine during its horizontal excavation period is 1.0802 m^3/min. Field measurement confirmed that gas emission obtained using the prediction model is slightly higher with an error rate of 4.67%. With such a small error rate and high safety, this model is suitable for the easy and rapid prediction of the amount of gas emitted from the floor coalbed.

3) From the point view of gas adsorption-desorption from coal seams, the finite element numerical simulation method was used to analyze the gas pressure relief behaviors in different mining stages during the sublevel excavation process. Based on the method, the predicted gas emission is 1.07 m^3/min. Quantitative analyses of gas desorption range of coal bodies in the coalbed at different moments indicated that the gas pressure-relief range is within 30 min in the floor coalbed. Field measurement confirmed that the numerical simulation is accurate and only slightly higher than the actual emission with an error rate of 3.68%. With high accuracy and safety, this numerical simulation method is suitable for predicting gas emission from the coalbed of SIETCS.

Acknowledgements: The authors gratefully acknowledge the financial supports by National Natural Science Foundation of China (Project No. 51674158、51974176 and 51474106) and Major Program of Shandong Province Natural Science Foundation (Project No. ZR2018ZA0602)，and the Taishan Scholar Talent Team Support Plan for Advantaged & Unique Discipline Areas

References

1 Tutak, M.; Brodny, J. Analysis of the Impact of Auxiliary Ventilation Equipment on the Distribution and Concentration of Methane in the Tailgate. *Energies* **2018**, *11*, 3076.
2 Tong, Ruipeng, et al. "Risk Assessment of Miners' Unsafe Behaviors: A Case Study of Gas Explosion Accidents in Coal Mine, China." International journal of environmental research and public health 16.10 (2019): 1765.
3 Wang, Gang, et al. "Deformation and gas flow characteristics of coal-like materials under triaxial stress conditions." *International Journal of Rock Mechanics and Mining Sciences* 91 (2017): 72-80.

4 Yang, Z., & Zhou, S. (2015). Modeling and prediction of daily gas concentration variation at a mining face based on the elliptic orbit model: A case study. *International Journal of Mining Science and Technology*, 25(6), 1045-1052.

5 Song, Yawei, et al. (2019) "Prediction of gas and coal spontaneous combustion coexisting disaster through the chaotic characteristic analysis of gas indexes in goaf gas extraction." Process Safety and Environmental Protection.

6 Karacan, C. Özgen, and Peter D. Warwick. "Assessment of coal mine methane (CMM) and abandoned mine methane (AMM) resource potential of longwall mine panels: Example from Northern Appalachian Basin, USA." International Journal of Coal Geology 208 (2019): 37-53.

7 Pramod Thakur. Advanced Mine Ventilation, 1rd ed.; Woodhead Publishing, USA, 2019; pp. 213-226.

8 Li, Zhen, et al. "The correlation between crushed coal porosity and permeability under various methane pressure gradients: a case study using Jincheng anthracite." Greenhouse Gases: Science and Technology 8.3 (2018): 493-509.

9 Cheng, Liu, Li Shugang, and Yang Shouguo. "Gas emission quantity prediction and drainage technology of steeply inclined and extremely thick coal seams." International Journal of Mining Science and Technology 28.3 (2018): 415-422

10 Salmachi, A., and J. Barkla. "Investigation of permeability change in the Bandanna Coal Formation of the Fairview Field using time-lapse pressure transient analysis." *The APPEA Journal* 59.1 (2019): 289-301.

11 Salmachi, Alireza, et al. "Investigation of permeability change in ultradeep coal seams using time-lapse pressure transient analysis: A pilot project in the Cooper Basin, Australia." *AAPG Bulletin* 103.1 (2019): 91-107.

12 Wang, Gang, et al. "Quantitative analysis of microscopic structure and gas seepage characteristics of low-rank coal based on CT three-dimensional reconstruction of CT images and fractal theory." *Fuel* 256 (2019): 115900.

13 Bi, J., & Jia, J. (2014). Prediction for gas emission quantity based on the compensation algorithm of PCMRA and neural network. J. *Nat. Disasters*, 23(5), 198-203.

14 Saghafi, A., Pinetown, K. L., Grobler, P. G., & Van Heerden, J. H. P. (2008). CO2 storage potential of South African coals and gas entrapment enhancement due to igneous intrusions. International *Journal of Coal Geology*, 73(1), 74-87.

15 Wang, L., Cheng, Y. P., Wang, L., Guo, P. K., & Li, W. (2012). Safety line method for the prediction of deep coal-seam gas pressure and its application in coal mines. *Safety science*, 50(3), 523-529.

16 Chen, L. , Wang, E. , Feng, J. , Kong, X. , Li, X. , & Zhang, Z. . (2016). A dynamic gas emission prediction model at the heading face and its engineering application. *Journal of Natural Gas Science and Engineering*, 30, 228-236.

17 Yang, L., & Liu, C. (2013). Prediction of Gas Emission Based on Partial Correlation Analysis and SVR. *Applied Mathematics & Information Sciences*, 7(5), 1671.

18 Wu, L., Liu, S., Chen, D., et al,.. (2014). Using gray model with fractional order accumulation to predict gas emission. *Natural hazards*, 71(3), 2231-2236.

19 Tutak, Magdalena, and Jarosław Brodny. "Predicting Methane Concentration in Longwall Regions Using Artificial Neural Networks." *International journal of environmental research and public health* 16.8 (2019): 1406.

20 Chen, S., Tang, D., Tao, S., Xu, H., Li, S., Zhao, J., ... & Li, Z. (2017). Characteristics of in-situ stress distribution and its significance on the coalbed methane (CBM) development in Fanzhuang-Zhengzhuang Block, Southern Qinshui Basin, China. *Journal of Petroleum Science and Engineering*, 161, 108-120.

21 Connell, L. D. (2009). Coupled flow and geomechanical processes during gas production from coal seams. *International Journal of Coal Geology*, 79(1-2), 18-28.

22 Cui, X., & Bustin, R. M. (2005). Volumetric strain associated with methane desorption and its impact on coalbed gas production from deep coal seams. *Aapg Bulletin*, 89(9), 1181-1202.

23 Shi, J. Q., & Durucan, S. (2005). A model for changes in coalbed permeability during primary and enhanced methane recovery. *SPE Reservoir Evaluation & Engineering*, 8(04), 291-299.

24 Palmer, I., Mavor, M., & Gunter, B. (2007, May). Permeability changes in coal seams during production and injection. In International Coalbed Methane Symposium, University of Alabama, *Tuscaloosa, Alabama.*,(0713).

25 Palmer, I., & Mansoori, J. (1998, January). How permeability depends on stress and pore pressure in coalbeds: a new model. In SPE annual technical conference and exhibition. *Society of Petroleum Engineers.*

26 Wu, Y., Liu, J., Elsworth, D., et al.. (2010). Dual poroelastic response of a coal seam to CO2 injection. International Journal of Greenhouse Gas Control, 4(4), 668-678.

27 Wang, G., Jiang, C., Shen, J., Han, D., & Qin, X. (2019). Deformation and water transport behaviors study of heterogenous coal using CT-based 3D simulation. International Journal of Coal Geology.

 doi:10.20944/preprints201909.0333.v1

28 Xia, T., Zhou, F., Liu, J., Hu, S., & Liu, Y. (2014). A fully coupled coal deformation and compositional flow model for the control of the pre-mining coal seam gas extraction. International Journal of Rock Mechanics and Mining Sciences, 72, 138-148.

29 Chen, Lianjun, and Guoming Liu. "Airflow-dust migration law and control technology under the simultaneous operations of shotcreting and drilling in roadways." Arabian Journal for Science and Engineering 44.5 (2019): 4961-4969.

30 Chen, Lianjun, et al. "Effect of pumping and spraying processes on the rheological properties and air content of wet-mix shotcrete with various admixtures." Construction and Building Materials 225 (2019): 311-323.

31 Ren, T., Wang, G., Cheng, Y., & Qi, Q. (2017). Model development and simulation study of the feasibility of enhancing gas drainage efficiency through nitrogen injection. Fuel, 194, 406-422.